Electronic Supplementary Material (ESI) for New Journal of Chemistry.
This journal is © The Royal Society of Chemistry and the Centre National de la Recherche Scientifique 2024

Supporting information

A cationic detergent based dye supramolecular assembly as unique turn-on probe for ATP

Fazil Fakhrul Hasan[a,1], Padma Nilaya Jonnalgadda[a, b,] Trilochan Gadly[c] and Goutam Chakraborty[a]*

[a]Laser and Plasma Technology Division, Bhabha Atomic Research Centre, Mumbai-400085.

[b]Homi Bhabha National Institute, Anushaktinagar, Mumbai-400094.

[c]Bio-Organic Division, Bhabha Atomic Research Centre, Mumbai-400085.

*Correspondence to: gchak@barc.gov.in (G. Chakraborty)

[1]On M.Sc research project from K. J. Somaiya College of Science and Commerce, Mumbai- 400077.

S.N.	Table of content	Page
1	**Experimental Section**	S3-S4
2	**Fig. S1. (A)** Normalized absorption and **(B)** normalized emission spectra of GEM-DNS@CTAB complex (20 μM GEM-DNS+0.25 mM CTAB) in different solvents.	S5
3	**Fig. S2. (A)** Absorption and **(B)** emission spectra of GEM-DNS@CTAB complex (20 μM GEM-DNS+0.25 mM CTAB) in different buffer solutions.	S5
4	**Fig. S3.** Variations in the fluorescence spectrum of GEM-DNS@CTAB complex (20 μM GEM-DNS+1.5 mM CTAB) in 5 mM tris buffer solution (pH ~7.4) at different concentrations of NaCl. Inset: Changes in emission intensity at 556 nm of GEM-DNS@CTAB complex with increasing NaCl concentration.	S6
5	**Fig. S4.** Normalized emission spectra of GEM-DNS@CTAB complex (20 μM GEM-DNS+0.25 mM CTAB) in 5 mM Tris buffer solution (pH ~7.4) at (1) 0 and (6) 74.8 μM ATP.	S6
6	**Fig. S5.** Excited-state decay traces of 20 μM GEM-DNS at (1) 0, (2) 0.25, (3) 0.40 and (4) 1.5 mM CTAB.	S7
7	**Fig. S6.** Anisotropy decay of 20 μM GEM-DNS at 0 (blue circles) and (2) 1.5 mM (green circles) CTAB.	S7
8	**Fig. S7.** Scanning electron microscopic (SEM) image of GEM-DNS@CTAB@ATP	S8

	ternary complex under different magnification.	
9	**Fig. S8.** Relative fluorescence responses of GEM-DNS@CTAB complex (20 μM GEM-DNS+0.25 mM CTAB) in 5 mM tris buffer solution (pH ~7.4) towards equi-molar concentration (30 μM) different biologically important analytes.	S8
10	**Fig. S9.** Relative absorption responses of GEM-DNS@CTAB complex (20 μM GEM-DNS+0.25 mM CTAB) in 5 mM tris buffer solution (pH ~7.4) towards equi-molar concentration (30 μM) different metal ions and biologically important analytes.	S9
11	**Fig. S10.** Fluorescence responses of GEM-DNS@CTAB complex (20 μM GEM-DNS+0.25 mM CTAB) in 5 mM tris buffer solution (pH ~7.4) towards equi-molar concentration (30 μM) of ATP (black) and BSA (red).	S9
12	**Fig. S11. (A)** Fluorescence spectra of GEM-DNS@CTAB complex (20 μM GEM-DNS+0.25 mM CTAB) with increase in concentration of ADP and (B) Comparative fluorescence responses of GEM-DNS@CTAB complex (20 μM GEM-DNS+0.25 mM CTAB) against concentration of ADP and ATP in 5 mM tris buffer solution (pH ~7.4).	S10
13	**Fig. S12.** Photographic image (from left to right) of free GEM-DNS (20 μM), GEM-DNS@CTAB binary complex (20 μM GEM-DNS+0.25 mM CTAB) and GEM-DNS@CTAB@ATP ternary complex (20 μM GEM-DNS+0.25 mM CTAB+75 μM ATP) in 5 mM tris buffer solution (pH ~7.4) under UV light irradiation (λ_{irr} ~365 nm).	S11
14	**Table S1.** Comparison of the performances of different fluorescent probes used for ATP detection.	S11-12
15	**References**	S12

1. EXPERIMENTAL SECTION

1.1 Materials and methods of sample preparation

Synthetically obtained GEM-DNS as reported in our previous work,[1] has been utilized in the present study. Concentrated stock solution of GEM-DNS in methanol has been diluted by tris buffer (5 mM, pH ~7.4) to make final concentration of the dye solution ~20 μM for our experiment. All the amino acids including inorganic salts, adenosine mono-phosphate (AMP) adenosine di-phosphate (ADP), tetrasodium pyrophosphate (PPi), adenosine tri-phosphate (ATP), urea, glucose, trypsin, lysozyme from chick egg white and cetyltrimethyl ammonium bromide (CTAB) were procured from SRL, India and were used as obtained. Human serum was obtained from Sigma-Aldrich and diluted to 0.25% (v/v) by 5 mM tris buffer solution prior using for our experiment.

1.2 Photophysical studies

A double beam UV-vis spectrophotometer (Model UV-2700, Shimadzu, Japan) was used to carry out all the ground-state absorption measurements in an optical quartz cell of path length 1 cm. A spectrofluorimeter (Model Fluoromax-4, Horiba, UK) was used for all steady-state (SS) fluorescence measurements where sample solutions taken in a 10 mm x 10 mm quartz cuvette were excited at 347 nm (isosbestic point) with a steady light beam. A time-correlated single photon counting (TCSPC) spectrometer obtained from Edinburgh, U.K was used to carry out the fluorescence lifetime measurements where the excitation source was a 405 nm pulsed diode laser (EPL-405) having pulse width of ~62 ps at 10 MHz pulse repetition rate. The time-resolved fluorescence decay traces for the samples were recorded at the emission maxima of free dye and dye@CTAB and dye@CTAB@ATP complexes at 592 nm and 548 nm respectively using a detection module based on photomultiplier tube (PMT). Light scattered by an aqueous suspension of ludox was used to obtain lamp profile and from the FWHM of recorded time profile, instrument response function (IRF) for this set up was measured to be ~250 ps. We maintained the magic angle (54.7 ^{o}C) configuration during recording of the excited state lifetime to avoid any anisotropy contribution from the decay profile.

A polyexponential function was used to fit the obtained decay traces,[2]

$$I(t) = I(0)\sum \alpha_i \exp(-t/\tau) \quad (1)$$

Average excited-state lifetime was calculated using equation,[2]

$$< \tau >= \sum A_i \tau_i \text{ where, } \quad A_i = \alpha_i \tau_i / \sum \alpha_i \tau_i \tag{2}$$

Time resolved anisotropy decay measurements were carried out using the same TCSPC setup where a 405 nm pulsed diode laser source, was used for excitation of the solutions. In these measurements, parallel and perpendicular polarized fluorescence decays, $I_{II}(t)$ and $I_{\perp}(t)$, were recorded independently, exciting the samples with vertically polarized light source. The anisotropy decay function r(t) was subsequently constructed as,[2]

$$r(t) = \frac{I_{II}(t) - GI_{\perp}(t)}{I_{II}(t) + 2GI_{\perp}(t)} \tag{3}$$

where G, is the correction factor for the polarization bias of the experimental set up. The G factor was independently estimated by measuring two perpendicularly polarized fluorescence decays, keeping the excitation light source horizontally polarized.[2]

1.3 Scanning electron microscopy (SEM)

Scanning electron microscope (Model: SEM-Carl Zeiss, Germany) was used to record SEM image of the GEM@CTAB@ATP complex. 10 μl of the sample was spotted on a clean glass slide and sputtered with gold using standard methods. An accelerating voltage of 10 keV used during scanning of the images for the GEM@CTAB@ATP samples.

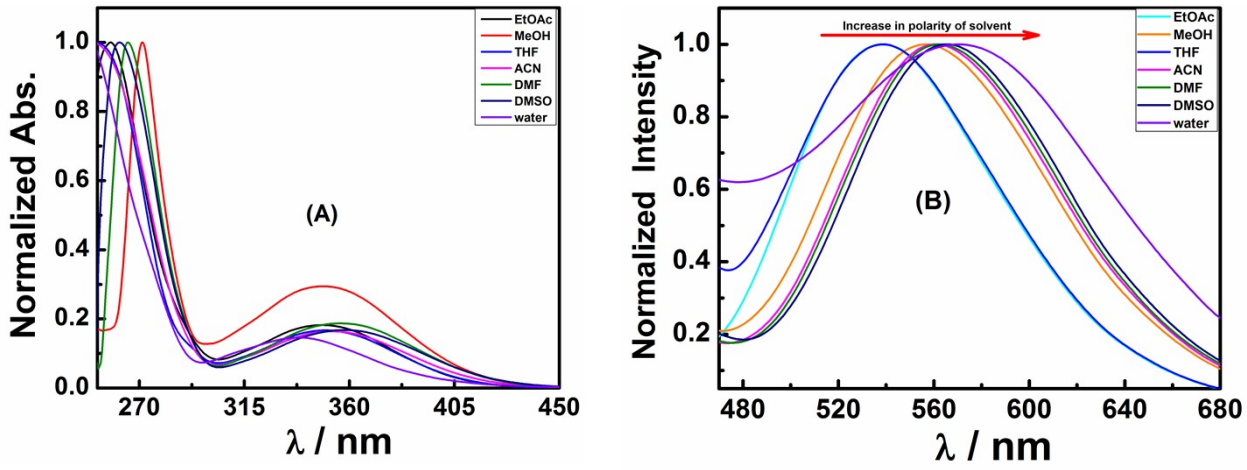

Fig. S1. (A) Normalized absorption and **(B)** normalized emission spectra of GEM-DNS@CTAB complex (20 μM GEM-DNS+0.25 mM CTAB) in different solvents. λ_{ex} = 347 nm.

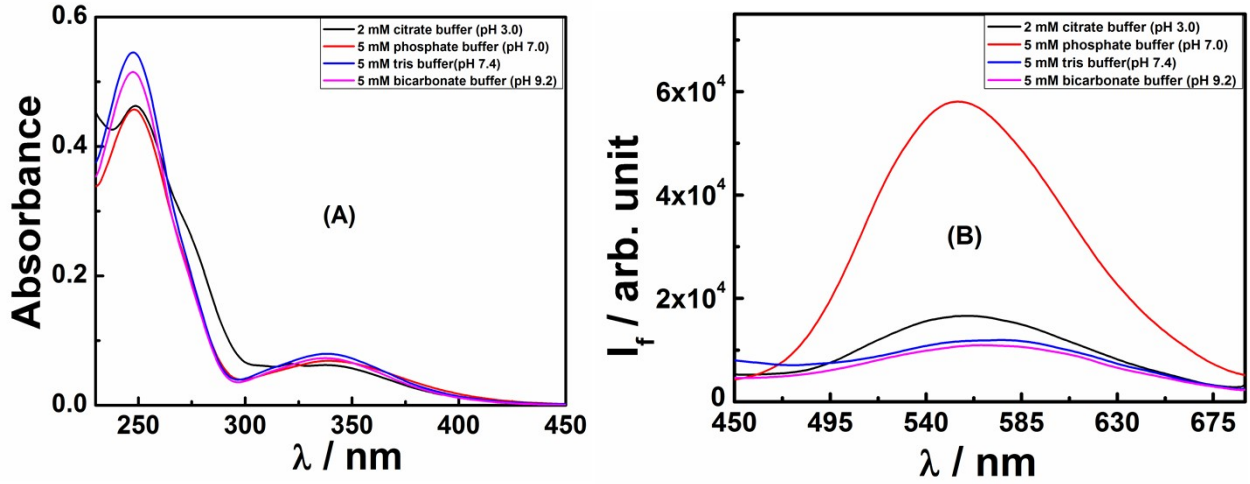

Fig. S2. (A) Absorption and **(B)** emission spectra of GEM-DNS@CTAB complex (20 μM GEM-DNS+0.25 mM CTAB) in different buffer solutions. λ_{ex} = 347 nm.

Explanation: Although the sensor assembly does not show any difference in absorption spectra in different buffer, the emission spectra of the sensory system display a different trend. It is obvious from figure S2B that emission intensity of the dye-surfactant assembly is significantly highly in phosphate buffer, providing large background signal during ATP detection. This makes 5 mM phosphate buffer unsuitable to be used in this study. On the other hand, based on low fluorescence background and free from any inorganic ion, we used tris buffer for ATP detection using GEM-DNS@CTAB complex.

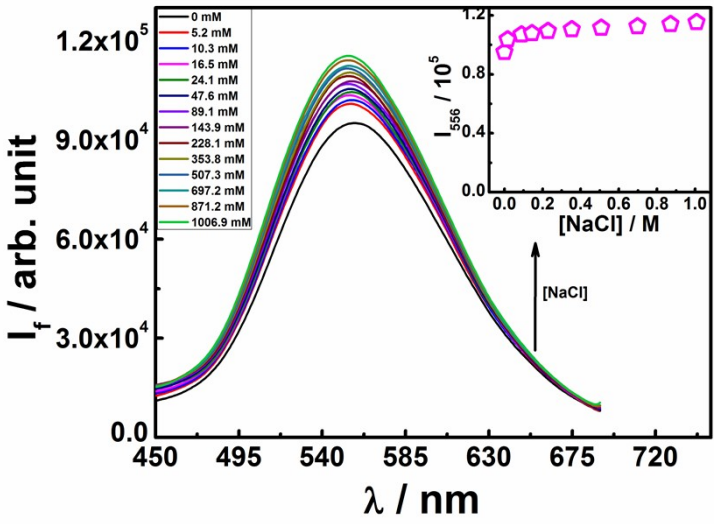

Fig. S3. Variations in the fluorescence spectrum of GEM-DNS@CTAB complex (20 μM GEM-DNS+1.5 mM CTAB) in 5 mM tris buffer solution (pH ~7.4) at different concentrations of NaCl. Inset: Changes in emission intensity at 556 nm of GEM-DNS@CTAB complex with increasing NaCl concentration. λ_{ex} = 347 nm.

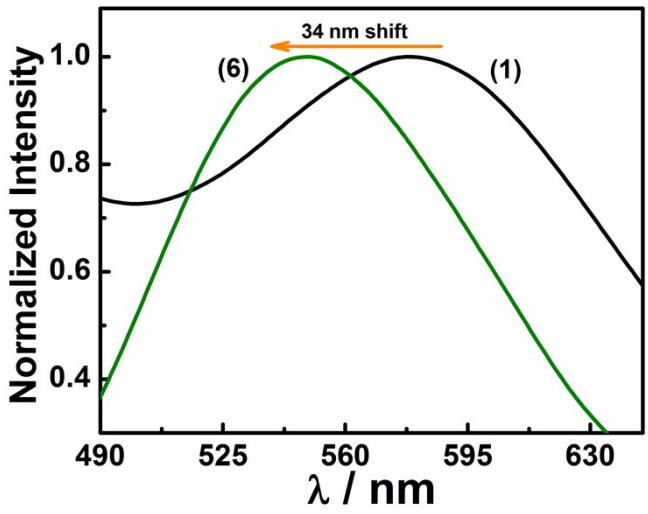

Fig. S4. Normalized emission spectra of GEM-DNS@CTAB complex (20 μM GEM-DNS+0.25 mM CTAB) in 5 mM Tris buffer solution (pH ~7.4) at (1) 0 and (6) 74.8 μM ATP. λ_{ex} = 347 nm.

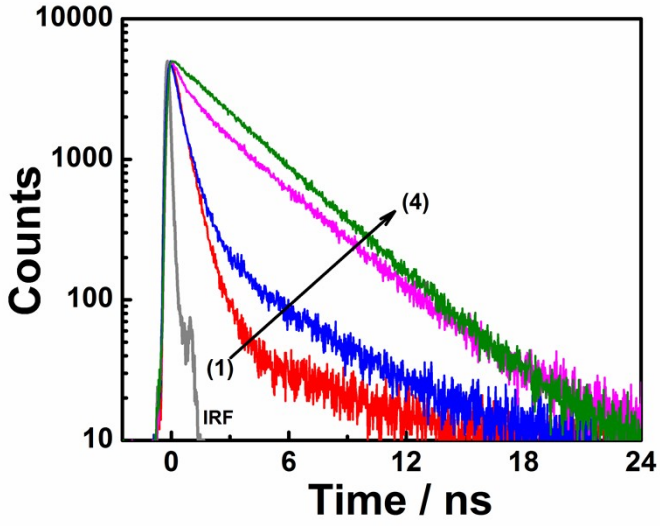

Fig. S5. Excited-state decay traces of 20 μM GEM-DNS at (1) 0, (2) 0.25, (3) 0.40 and (4) 1.5 mM CTAB. λ_{ex} = 405 nm.

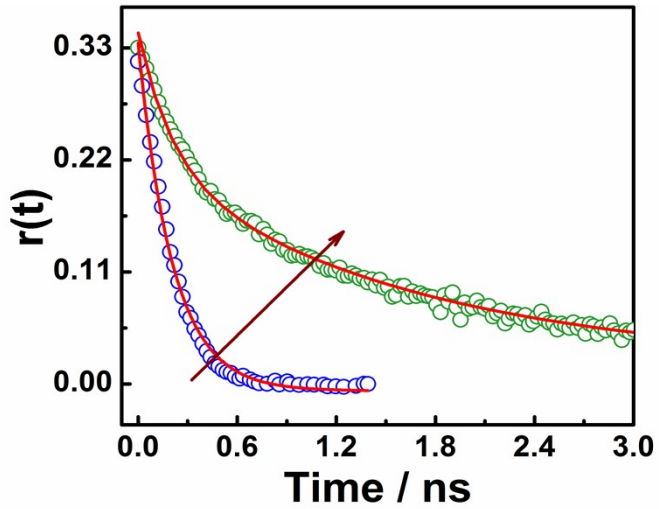

Fig. S6. Anisotropy decay of 20 μM GEM-DNS at 0 (blue circles) and (2) 1.5 mM (green circles) CTAB.

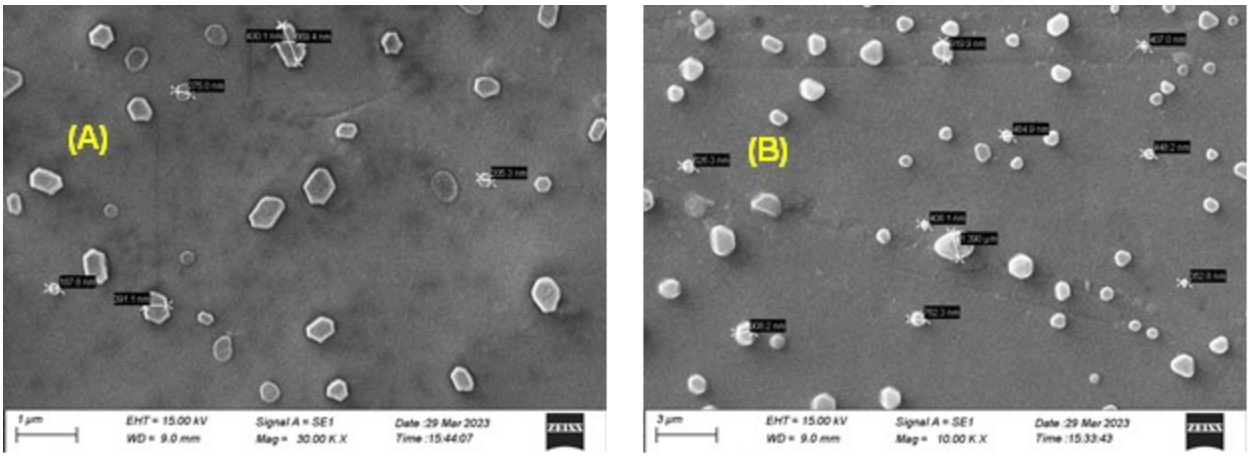

Fig. S7. Scanning electron microscopic (SEM) image of GEM-DNS@CTAB@ATP ternary complex under different magnification.

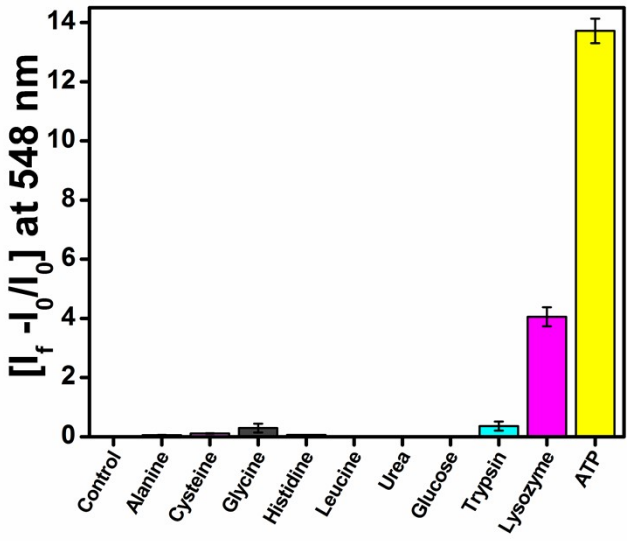

Fig. S8. Relative fluorescence responses of GEM-DNS@CTAB complex (20 μM GEM-DNS+0.25 mM CTAB) in 5 mM tris buffer solution (pH ~7.4) towards equi-molar concentration (30 μM) different biologically important analytes.

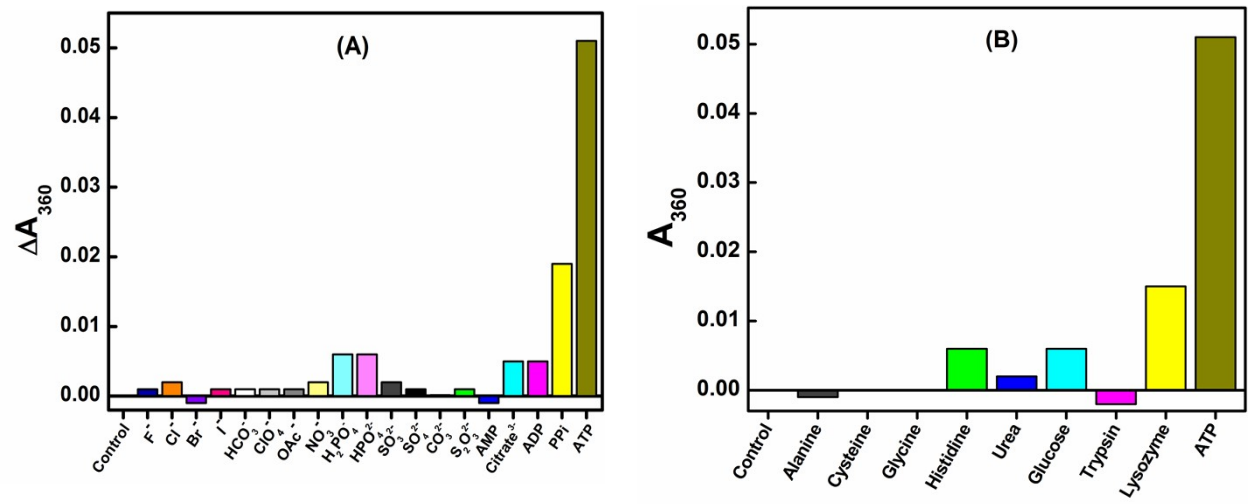

Fig. S9. Relative absorption responses of GEM-DNS@CTAB complex (20 μM GEM-DNS+0.25 mM CTAB) in 5 mM tris buffer solution (pH ~7.4) towards equi-molar concentration (30 μM) different metal ions and biologically important analytes.

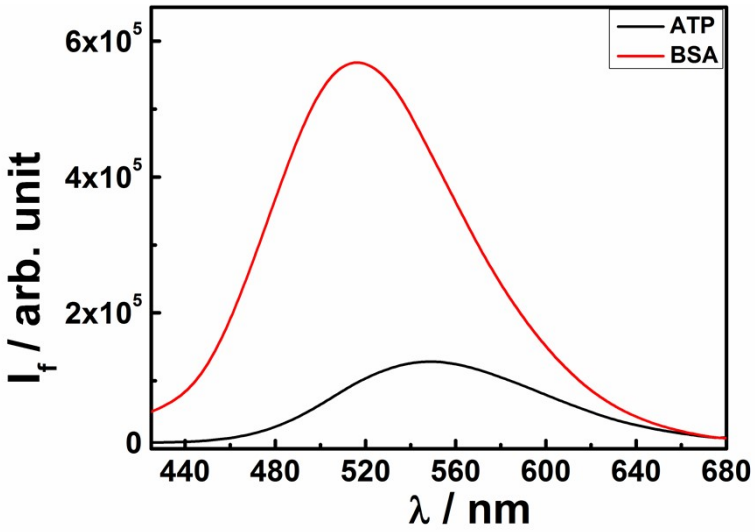

Fig. S10. Fluorescence responses of GEM-DNS@CTAB complex (20 μM GEM-DNS+0.25 mM CTAB) in 5 mM tris buffer solution (pH ~7.4) towards equi-molar concentration (30 μM) of ATP (black) and BSA (red).

Explanation: It has been observed that GEM-DNS@CTAB complex has significant response towards BSA (even more than ATP) mainly due to strong affinity of the GEM-DNS dye towards ATP.[1] This somewhat limits the use of this dye-surfactant assembly for the detection of ATP in

serum matrix. However, this problem can be mitigated by suitably diluting the serum matrix prior detection of ATP. This procedure has been adopted in our study by diluting serum matrix to 0.25%, although small background signal cannot be avoided.

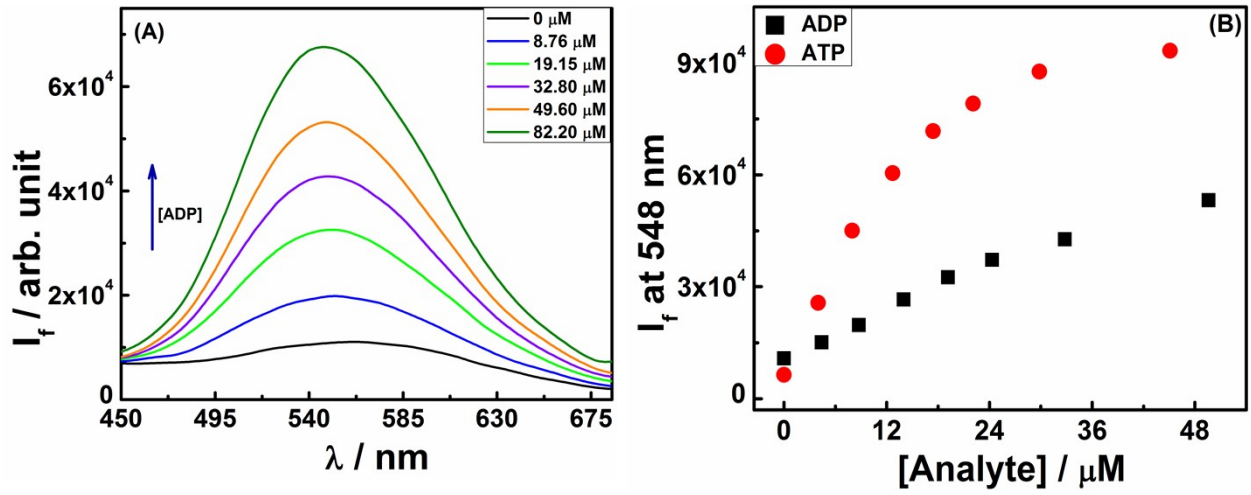

Fig. S11. (A) Fluorescence spectra of GEM-DNS@CTAB complex (20 μM GEM-DNS+0.25 mM CTAB) with increase in concentration of ADP and **(B)** Comparative fluorescence responses of GEM-DNS@CTAB complex (20 μM GEM-DNS+0.25 mM CTAB) against concentration of ADP and ATP in 5 mM tris buffer solution (pH ~7.4).

Explanation: ADP also has a high negative charge density. For this reason, ADP can also show large enhancement in fluorescence intensity at a higher concentration. However, concentration of ADP in biological media is significantly less than ATP and also due to lesser charge density the interference due ADP can be neglected. To show the effect of ADP and ATP on GEM-DNS@CTAB complex we have presented the comparative fluorescence enhancement plot for better understanding.

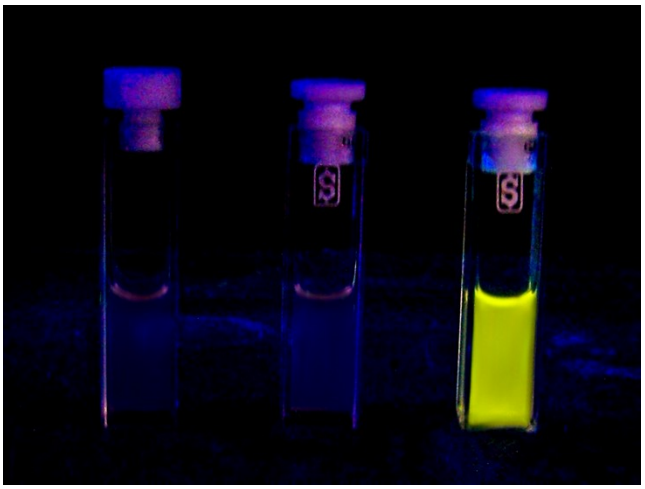

Fig. S12. Photographic image (from left to right) of free GEM-DNS (20 μM), GEM-DNS@CTAB binary complex (20 μM GEM-DNS+0.25 mM CTAB) and GEM-DNS@CTAB@ATP ternary complex (20 μM GEM-DNS+0.25 mM CTAB+75 μM ATP) in 5 mM tris buffer solution (pH ~7.4) under UV light irradiation (λ_{irr} ~365 nm).

Table S1. Comparison of the performances of different fluorescent probes used for ATP detection.

S.N.	Probe	Mode of operation Technique	Linearity Range	LOD	Ref.
1	DSAI	Turn-On	0.1-5 μM	32.8 nM	3
2	TPE-COOH/Cu^{2+} complex	Turn-On	0-20 μM	42.3 nM	4
3	Quaternary ammonium silole	Turn-On	0-7 μM	69 nM	5
4	Zn coordinated AgNCs/GSH	Turn-Off	1–110 μM	0.8 μM	6
5	N-(Anthracen-9'-yl-methyl)tris(3-aminopropyl)amine	Turn-On	0.5–100 ppm	1 μM	7
6	ANS-PAMA complex	Turn-Off	0–28 μM	1.5 μM	8

7	BBR-SBE_{10}βCD-Cd^{2+} complex	Turn-On	51–630 μM	18 μM	9
8	DNA aptamer with cationic tetrahedralfluorene	Turn-Off	0-300 μM	20 μM	10
9	Silica nano particle based aptamer	Turn-Off	0–200 μM	20 μM	11
10	GEM-DNS@CTAB complex	Turn-On	0–4.5 μM	0.25 μM	**This study**

References

1. T. Gadly, B. S. Patro and G. Chakraborty, *Colloids Surf., B*, 2022, **220**, 112865.
2. J. R. Lakowicz, *Principles of Fluorescence Spectroscopy*. 3rd Edition, Plenumm Press, Springer, New York, 2006.
3. H. Li, Z. Guo, W. Xie, W. Sun, S. Ji, J. Tian and L. Lv, *Anal. Biochem.*, 2019, **578**.
4. L.-Y. Geng, Y. Zhao, E. Kamya, J.-T. Guo, B. Sun, Y.-K. Feng, M.-F. Zhu and X.-K. Ren, *J. Mater. Chem. C*, 2019, **7**, 2640-2645.
5. M. Zhao, M. Wang, H. Liu, D. Liu, G. Zhang, D. Zhang and D. Zhu, *Langmuir*, 2009, **25**, 676-678.
6. X. Liu, Y. Yu, B. Lin, Y. Cao and M. Guo, *Spectrochim. Acta, Part A*, 2019, **214**, 360-365.
7. G. P. Foy and G. E. Pacey, *Talanta*, 1996, **43**, 225–232.
8. D. K. Mal, P. N. Jonnalgadda, R. K. Chittela and G. Chakraborty, *J. Mol. Liq.*, 2023, **376**, 121402.
9. G. Chakraborty, R. K. Chittela, P. N. Jonnalgadda and H. Pal, *J. Mol. Liq.*, 2022, **359**, 119316.
10. Y. Wang and B. Liu, *Analyst*, 2008, **133**, 1593–1598.
11. L. Cai, Z.-Z. Chen, X.-M. Dong, H.-W. Tang and D.-W. Pang, *Biosens Bioelectron.*, 2011, **29** 46–52.